JOC The Journal of Organic Chemistry

Article

pubs.acs.org/joc

# Pd(OAc)$_2$-Catalyzed C−H Activation/C−O Cyclization: Mechanism, Role of Oxidant—Probed by Density Functional Theory

Bing Lian,[†] Lei Zhang,[†] Gregory Adam Chass,[‡] and De-Cai Fang*,[†]

[†]Key Laboratory of Theoretical and Computational Photochemistry, Ministry of Education, College of Chemistry, Beijing Normal University, Beijing 100875, China

[‡]School of Biological and Chemical Sciences, Queen Mary University of London, London, E1 4NS, U.K.

Supporting Information

**ABSTRACT:** A series of density functional theory determinations have been carried out to characterize Pd(OAc)$_2$-catalyzed C−H activation and subsequent intramolecular C−O bond-coupling of phenyl-*tert*-butanol in perfluorobenzene ($C_6F_6$) solvent. Full, nontruncated models of the real chemical transformations were studied, with structures in agreement with recent X-ray determinations. Conformational analyses have provided thermodynamic validity of the geometric structures used. The B3LYP/DZVP and B3LYP/BS1 methods (BS1 = TZVP$_{(H,C,O)}$ + SDD$_{(Pd,I)}$) were comparatively employed, with $C_6F_6$ solvent contributions accounted for by the IDSCRF method; key transition states were confirmed by intrinsic reaction coordinate determinations. The novel reaction mechanism proposed was divided into the following four steps: C−H activation, oxidation, reductive elimination, catalyst recovery. Two competing reaction routes were quantitatively compared, differing in the oxidation state of Pd (+2 vs +4). Results reveal the pathway involving Pd(IV) intermediates to be more spontaneous and, therefore, more probable than the Pd(II) path, the latter hindered by a kinetically inaccessible reductive elimination step, with total energy and free energy barriers of 41.0 and 38.6 kcal·mol$^{-1}$, respectively. The roles played by the oxidant and Pd(IV) species have also been addressed through Bader's atoms-in-molecules wave function analyses, providing a quantitative electronic metric for C−H activation chemistry.

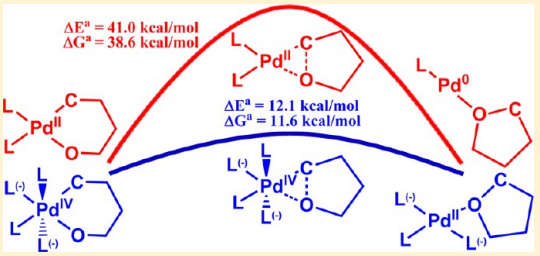


## 1. INTRODUCTION

Transition-metal-catalyzed C−H activation has experienced enormous growth in the past decade, and represents evolution of a fundamental aspect of modern synthetic chemistry,[1] with significant application to construction of carbon−carbon or carbon−heteroatom bonds.[2] It provides an efficient and shortened alternative to multistep synthetic C−H functionalizations, and together with its high atom economy represents a major driving force in green and enabling chemistry.[3]C−H activation represents the central research focus of recent impacting works.[4]Efforts are presently directed to the expansion of substrate-scope,[5] exploration of novel ligands with high efficiency and particular reactivity,[6]characterizing the roles of catalytic species,[7] and rational control of regio- and stereoselectivity.[8]

Parallel development of palladium catalysis in organometallic chemistry has resulted in many coupling reactions now being used in the production of pharmaceutical compounds, natural products, polymers, and conjugated organic materials.[3a,9]These transformations provide effective means for the direct coupling of an unactivated C−H bond with a variety of partners, specifically, C−C, C−N, C−S, and C−O bond-coupling through direct C−H activation catalyzed by Pd complexes,[3−6,10] with particular focus on heteroatom-containing partners.

Among these, the catalyzed C−H activation/C−O bond-couplings have been extensively studied and refined in recent years because of their important applications to construction of synthetically valuable organic moieties and synthetic frameworks. Although previous experimental[2−4,10,11] and computational[12] studies have addressed some mechanistic aspects of these reactions, it is still unclear what quantitative role the oxidants play and whether or not a Pd(IV) species[3a,13] is involved. Most recently, Sanford and co-workers reported a C−H activation involving Pd(IV) centers.[13k] This work involved the synthesis of a Pd(IV) complex from a Pd(II) precursor and $PhICl_2$ (oxidant) at the low temperatures (243 K), with subsequent characterization of the oxidant product by X-ray diffraction, showing a six-coordinate ligand field structure.

In 2010, Wang and co-workers[14] reported a new synthetic method for the Pd(OAc)$_2$-catalyzed construction of a substituted dihydrobenzofuran system (**3a**) from phenyl-*tert*-butanol (**1a**) via a C−H activation/C−O bond-coupling directed by the hydroxyl group (Scheme 1).

Experiments showed 1.5 equiv of oxidant PhI(OAc)$_2$ (**2a**) (in the presence of $Li_2CO_3$ base) generated the desired product (**3a**) in good yield (88%), while modulation of the oxidant (**2a**) with PhI(TFA)$_2$ (**2b**) or PhI(OPiv)$_2$ (**2c**) reduced the reaction

**Received:** May 15, 2013
**Published:** July 24, 2013

   dx.doi.org/10.1021/jo4010712 | J. Org. Chem. 2013, 78, 8376−8385

**Scheme 1. Pd(OAc)$_2$-Catalyzed C−H Activation/C−O Cyclization of Phenyl-*tert*-butanol (1a) in $C_6F_6$ Solvent, Characterized in This Work**

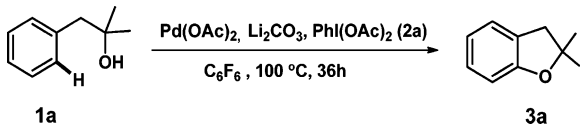


yield to 13% or 50%, respectively. A number of moderate oxidants, such as silver and copper salts, gave complete recovery of starting material. On this basis, these authors assumed that the catalyzed reaction may proceed via a Pd(IV) intermediate "keystone" supporting a Pd(II) → Pd(IV) → Pd(II) pathway, in direct contrast to the more widely accepted Pd(II) → Pd(0) → Pd(II) route. However, neither experimental nor theoretical evidence exists to support the significance of a Pd(IV) intermediate—until now.

Toward resolving this mechanistic dichotomy, we carried out a series of density function theory (DFT)[15]determinations toward quantitatively characterizing the detailed mechanism of the C−H activation/C−O coupling reaction (Scheme 1), with focus on the role of oxidant and the competing oxidation states of Pd.

The optimized geometries of all possible stationary points, kinetic and thermodynamic aspects of the proposed catalytic cycles, and roles of oxidant and Pd(IV) species are discussed in this work, complemented by high-level electronic structure analyses comparing the $Pd^{(II)\rightarrow(IV)\rightarrow(II)}$ and $Pd^{(II)\rightarrow(0)\rightarrow(II)}$ pathways. It is our belief that the systematic approach herein will provide an evolved methodological approach and insight into the structure and mechanisms for C−H activation processes.

## 2. RESULTS AND DISCUSSION

Results presented within this involve characterization of the overall reaction equation in Scheme 1. Focus was on characterization of intramolecular C−O bond formation, which proceeds via deprotonation of two H atoms by base. Therein, a hydroxyl group in the $\beta$-position to the phenyl ring in the substrate forms a five-membered ring structure through successive C−H activation and C−O bond-coupling.

The proposed reaction pathway in this study is divided into the following segments of the full chemical transformation: C−H activation, oxidation, reductive elimination (RE), and catalyst recovery (CR), labeled as steps 1−4, respectively (Scheme 2a).

Scheme 2 only presents the general picture of the reaction mechanism, as the four steps are themselves composed of elementary substeps, each explicitly addressed in the following sections. Results reported throughout are based on the B3LYP +IDSCRF/DZVP method, with all free energies determined at the experimental reaction temperature (373 K), except where noted.

**Scheme 2. Schematic Depiction of the Entire Catalytic Cycle of the C−H Activation/C−O Coupling Reaction**

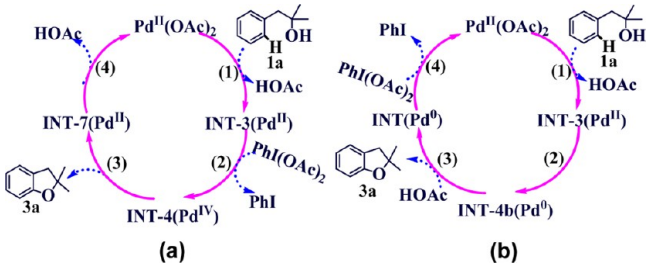


### 2.1. Conformational Analysis of Substrate Geometry.

A preliminary and requisite conformational analysis of the phenyl-*tert*-butanol substrate's structure was carried out to ensure thermodynamic validity for the geometries used in the mechanism. The two rotatable C−C single bonds (C2−C3 and C3−C4) afford only two stable rotamers for the C2−C3−C4−O1 dihedral angle ($\theta_1$), which adopts either a *gauche*$^+$ (58.0°) or an *anti* (177.8°) conformation, labeled **1a** and **1b**, respectively (Scheme 3). The C4−C3−C2−C6 dihedral angle ($\theta_1$) remains at ∼90° in both **1a** and **1b** conformers, signifying a requisite perpendicularity of the C3−C4 bond with respect to the phenyl plane.

**Scheme 3. Structures, Selected Dihedral Angle Parameters, Relative Total Energies, and Free Energies (kcal·mol$^{-1}$) of Stable Conformations of Phenyl-*tert*-butanol**

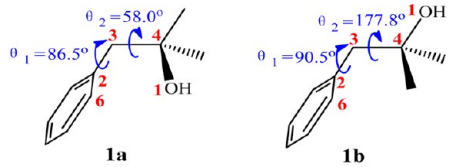


| | 1a | 1b |
|---|---|---|
| ΔE | 0.0 | 1.2 |
| ΔG | 0.0 | 1.1 |

The relative total energy (electronic energy + zero-point energy) and relative Gibbs free energy show **1a** to be ∼1.2 kcal·mol$^{-1}$ more stable than **1b**; hence, **1a** dominates the equilibrium concentration. The C4−O1 bond, thus the hydroxyl group, adopts a *gauche* orientation relative to the phenyl group in **1a**, placing the Pd center proximal to the C6−H bond in the substrate−catalyst complex. As C−H activation benefits from the complex-induced proximity effect (CIPE),[16] we concluded that **1a** is the most reactive conformation in the present study, hence unambiguously referred to as such throughout this work. Adding to the conformational certainty is the observation that the C4−O1 bond in **1b** arranges *anti*-parallel to the C2−C3 bond, placing the hydroxyl group at a large distance from the C6−H bond, negating any potential for CIPE contributions.

**2.2. Reaction Mechanism and Energy Profile.** The proposed reaction mechanism for the entire catalytic cycle is depicted in Figure 1, replete with geometric structures and the atomic numbering system used; this is complemented by an energetic "roadmap" in Figure 2.

The first step of the mechanism, common to other transition-metal-catalyzed reactions,[3a] involves a substrate−catalyst encounter and combination mediated by a ligand exchange, involving the hydroxyl O1 atom of **1a** and the O2 atom of one of the $\eta^2$-$CH_3COO^-$ ligands. The corresponding transition state **TS-1** displays the concerted nature of this process, with the interatomic distances of the Pd···O1 and Pd···O2 incipient bonds being 2.63 and 2.45 Å, respectively, subsequently relaxing to a four-coordinate square intermediate **INT-1**. This process is assisted by an O1−H···O2 H-bond between **1a** and $Pd(OAc)_2$, strengthened along the reaction coordinates evidenced by the significant shortening of the H···O2 distance on moving from **TS-1** (2.15 Å) to **INT-1** (1.46 Å).


dx.doi.org/10.1021/jo4010712 | J. Org. Chem. 2013, 78, 8376−8385

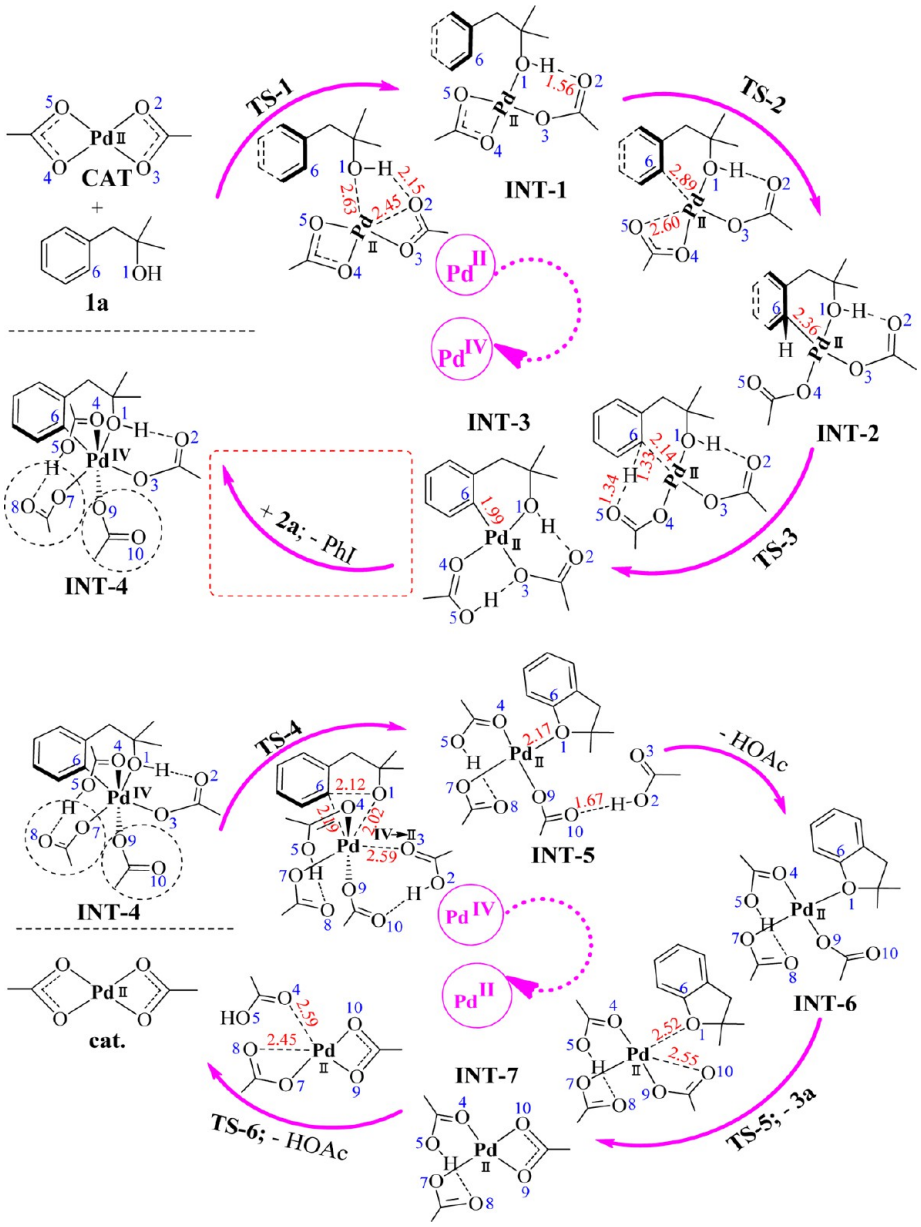


**Figure 1.** Proposed reaction mechanism for the entire catalytic cycle along the Pd(II) → Pd(IV) → Pd(II) reaction profile. Depictions of the structures residing at critical points, geometry-optimized at the B3LYP+IDSCRF/DZVP level of theory, are provided in addition to the atomic numbering system used. Partially formed and cleaved bonds in transition states are represented by dashed lines, with selected interatomic distances (in Å) shown in red text. With the exception of the INT-3($Pd^{II}$) → INT-4($Pd^{IV}$) → INT-5($Pd^{II}$) steps involving an oxidation state change, the formal charge on Pd is +2 throughout the cycle (e.g., INT-3 has one neutral and two (−1) ligands (O4-based neutral acetic acid and O3-based acetate anion, bidentate substrate, respectively).

This is followed by an intramolecular ligand substitution via concerted exchange of the O5 atom in the arm of the second $\eta^2$-$CH_3COO^-$ ligand with the C6 atom on the phenyl group, generating an intermediate bearing two $\eta^1$-$CH_3COO^-$ groups in the ligand field (**INT-2**). The Pd−C6 bond axis in **INT-2** orientates itself perpendicular to the phenyl plane, indicative of a Pd−$\pi$ interaction (Pd···C = 2.36 Å), through which the H atom on the C6 center is brought within 2.35 Å of the O5 atom in preparation for C−H activation.

The H atom on the C6 center could be abstracted by the *cis*-acetate O5 atom through the six-membered ring transition structure **TS-3**, a typical hydrogen-transfer transition state, with the distances of O5···H and H···C6 being 1.34 and 1.33 Å, respectively. The Pd···C6 incipient bond in **TS-3** is coplanar with the phenyl plane and aligned with the $sp^2$-hybrid orbital on the C6 center, signifying a Pd−$\pi$ → Pd−C $\sigma$-bond conversion, concomitant with substantial bond strengthening; similar six-membered ring transition structures have been reported in related works.[12a−d] Geometric relaxation of **TS-3** along the reaction route generates the C−H activation intermediate product (**INT-3**), itself displaying a six-membered cyclopalladated intermediate with two stabilizing O−H···OH bonds.

An oxidative $PhI(OAc)_2$ molecule (**2a**) is able to easily oxidize **INT-3**, through addition of two acetate groups to the Pd center, to a six-coordinate octahedral Pd(IV) complex (**INT-4**), simultaneously releasing the reduction product (PhI) to solution (**INT-3** + **2a** → **INT-4** + PhI). Calculations show that it is a free energy favorable process ($\Delta G_{dzvp}$ = −1.2 kcal·


dx.doi.org/10.1021/jo4010712 | J. Org. Chem. 2013, 78, 8376−8385

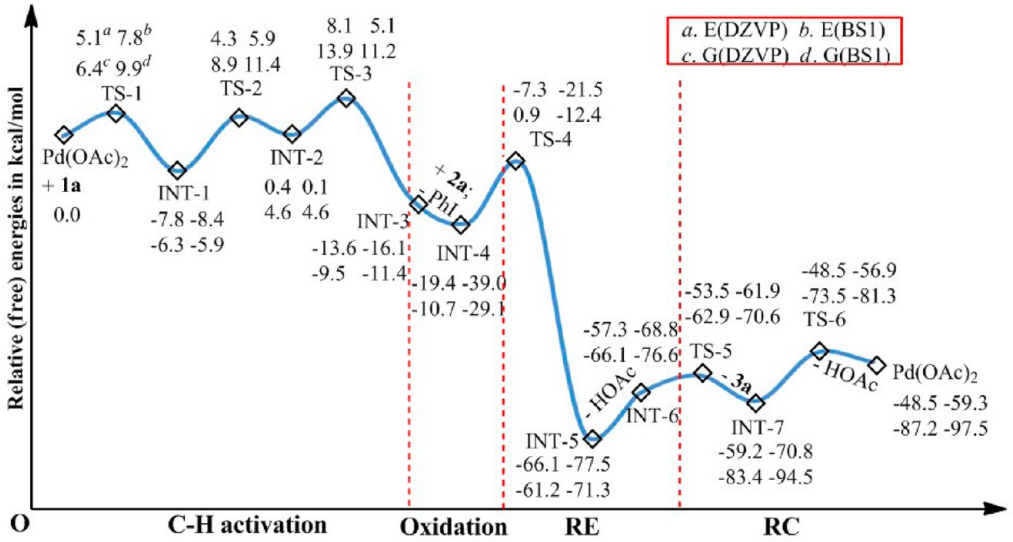


**Figure 2.** Relative total energy (electronic + ZPE) and Gibbs free energy profiles (kcal·mol$^{-1}$) for the entire $Pd(OAc)_2$-catalyzed transformation of phenyl-*tert*-butanol (**1a**) to dihydrobenzofuran (**3a**), as determined at the B3LYP+IDSCRF/DZVP (*left-hand values*) and B3LYP+IDSCRF/BS1 (*right-hand values*) levels of theory.

mol$^{-1}$ and $\Delta G_{BS1}$ = −17.7 kcal·mol$^{-1}$) and consists of multiple elementary steps; details of this process are discussed in section 2.4.

The Pd−C6 and Pd−O1 bonds in **INT-4** are *ortho* to one another, which is favorable for RE via a three-membered ring transition state (**TS-4**), forming a four-coordinate square intermediate (**INT-5**), concurrently recovering the Pd's + 2 oxidation state [Pd(IV) → Pd(II)]. The intramolecular C−O bond-coupling in **TS-4** is accompanied by a Pd−O3 bond cleavage, affording the square ligand configuration. The hydroxyl group undergoes a deprotonation event through the O1 → O2 H transfer in a concerted, but nonsynchronous, manner with C−O bond-making. Following this step, direct rupture of the neutral acetic acid, being H-bonded to the O10 atom, affords an intermediate (**INT-6**) without any transition state.

Intrinsic reaction coordinate (IRC) results, linking the two minima on either side of **TS-4**, have confirmed that the product (**3a**) is still bound to the Pd center (**INT-6**). An intramolecular substitution mediated by the O10 atom of the $\eta^1$-$CH_3COO^-$ ligand could remove **3a** from the Pd center via the **TS-5** transition structure, itself followed by another intramolecular substitution with the O8 atom of the $\eta^1$-$CH_3COO^-$ ligand replacing the acetic acid O4 atom, regenerating the $Pd(OAc)_2$ catalyst.

The total energy and free energy profiles are provided in Figure 2, for both levels of theory investigated, specifically, the B3LYP+IDSCRF/DZVP and B3LYP+IDSCRF/BS1 levels (see the Computational Details section). It should be noted that the free energy changes of the bimolecular reaction processes reported were determined relative to the weakly bound bimolecular complexes as references. This is in direct contrast to the commonly used reference, derived from the sum of the separate molecules.

Results revealed that the first two ligand exchanges should proceed easily with energy barriers of 5.1 and 12.1 kcal·mol$^{-1}$, and free energy barriers of 6.4 and 15.2 kcal·mol$^{-1}$, respectively. The latter is kinetically disfavored (with respect to relatively free energy), as the entering ligand (C6 atom) is a poor coordinating atom with respect to the leaving ligand (O5 atom). The proton-abstraction step (**INT-2** → **TS-3** → **INT-3**) involves an energy barrier of only 7.7 kcal·mol$^{-1}$ and a free energy barrier of 9.3 kcal·mol$^{-1}$, readily accessible at the experimental temperature used (373 K).This proceeds via **TS-3**, wherein the H atom on C6 transfers to O5, changing the O4-based ligand to a neutral acetic acid ligand. The acidic proton on O5 forms a H-bond with a nearby electronegative atom (O3 in this case = O5−H···O3). This was confirmed by IRC calculations tracking the transformation in both the forward and the backward directions. Therein, the relaxation of **TS-3** in the forward direction (**TS-3** → **INT-3**) was accompanied by rotation of the Pd−O4 bond to form the O5−H···O3 H-bond.

The intermediate product formed (**INT-3**) favorable in relative energy, as the $Pd(OAc)_2$ + **1a** → **INT-3** transformation is exergonic by −13.6 kcal·mol$^{-1}$ energy and −9.5 kcal·mol$^{-1}$ free energy, which is stabilized by two intramolecular O···H−O H-bonds. Results are similar for both levels of theory (B3LYP +IDSCRF/DZVP and B3LYP+IDSCRF/BS1) for the C−H activation process.

However, the energetic profile of the oxidation reaction process converting **INT-3** to **INT-4** shows wide variation with level of theory, determined to be −5.8 and −22.9 kcal·mol$^{-1}$ energy and −1.2 and −17.7 kcal·mol$^{-1}$ free energy, for the B3LYP+IDSCRF/DZVP and B3LYP+IDSCRF/BS1 levels, respectively. This observed basis set effect may be attributed to the relatively stronger (or shorter) coordinating bonds predicted by the theoretically inferior BS1 basis set. Hence, the increase of coordination number in the **INT-3** → **INT-4** process would be accompanied by a greater exergonic energy estimated by BS1, with respect to that predicted by DZVP.

This rationale could also be used to account for the inverse basis set effect observed for the C−O RE process (**INT-4** → **TS-4** → **INT-5**), which involves a decrease of coordination number, where BS1 predicts a higher energy barrier [$\Delta\Delta E_a^{\ddagger}$ = $17.5_{BS1}$ − $12.1_{DZVP}$ = +5.4 kcal·mol$^{-1}$] and lower exergonic reaction energy than the DZVP level [$\Delta\Delta E_r$ = ($-38.5_{BS1}$) − ($-46.7_{DZVP}$) = +8.2 kcal·mol$^{-1}$]. When the $Pd(OAc)_2$ catalyst is regenerated, an extra 26.0 kcal·mol$^{-1}$ free energy will be liberated, contributing to an extremely exergonic transformation ($\Delta E_{dzvp}$ = −48.5 kcal·mol$^{-1}$, $\Delta G_{dzvp}$ = −87.2 kcal·


dx.doi.org/10.1021/jo4010712 | J. Org. Chem. 2013, 78, 8376−8385

$mol^{-1}$ and $\Delta E_{BS1}$ = −59.3 kcal·$mol^{-1}$, $\Delta G_{BS1}$ = −97.5 kcal·$mol^{-1}$).

Despite the **INT5** → **INT6** + $CH_3COOH$ transformation being energetically unfavorable (+8.8 kcal·$mol^{-1}$), it is favorable in free energy (−4.9 kcal·$mol^{-1}$) due to the release of acetic acid into solution. However, as the concentration of acetic acid in solution grows, the reaction equilibrium may be shifted to favor the reverse process (regenerating **INT5**), retarding release of product (**3a**) from its Pd ligand site; a mere 46% product yield was observed in the absence of base. The introduction of salt ($Li_2CO_3$ or $Na_2CO_3$) facilitates formation of complex **COM-M** (M = Li or Na), helping disassociate acetic acid from **INT-5** (Figure 3, *left-hand side*). Therein, the strong O10···H−O hydrogen bond is completely destroyed, leaving a vacancy on Pd for O10 to attack and promote release of the product (**3a**). Modification of the complex's configuration to that of **COM-K** (Figure 3, *right-hand side*), wherein a K atom is connected to O2, results in a shortening of the O2−H···O10 hydrogen bond found in **INT-5** (1.67 Å → 1.62 Å) (see Figure 1). A more detailed dissemination of this is provided in the Supporting Information.

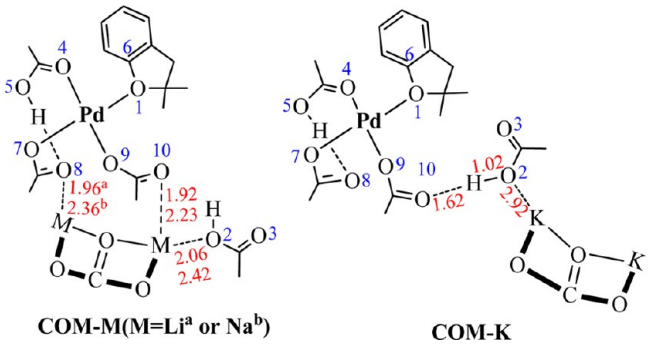


**Figure 3.** Two differing structural configurations for complexes formed between **INT5** and $M_2CO_3$, where M = Li, Na, or K.

**2.3. Comparison of $Pd^{(II)\rightarrow(IV)\rightarrow(II)}$ and $Pd^{(II)\rightarrow(0)\rightarrow(II)}$ Catalytic Cycles.** The reaction mechanism characterized and discussed in the previous section2.2 involves two changes of oxidation state at the Pd center: Pd(II) → Pd(IV) through an oxidation process and Pd(IV) → Pd(II) via a C−O RE process, representing an overall Pd(II) → Pd(IV) → Pd(II) cycle. For sake of comparison, the more common Pd(II) → Pd(0) → Pd(II) cycle was also similarly characterized, wherein the C−O RE process transforming Pd(II) to Pd(0) precedes the oxidation process, itself involving an oxidative $PhI(OAc)_2$ molecule (**2a**) facilitating recovery of the $Pd(OAc)_2$ catalyst [Pd(0) → Pd(II)] (see Scheme 2b).

Toward estimating the relative energy demands of the two pathways, the C−O RE process starting from the Pd(II) complex (**INT-3**) has been characterized and compared to that of the Pd(IV) complex (**INT-4**). Our DFT determinations show that the Pd(II) → Pd(0) reaction path (**INT-3** → **TS-3-b** → **INT-4-b**) needs to surmount an energy barrier and free energy barrier of 41.0 and 38.6 kcal·$mol^{-1}$, respectively, whereas the Pd(IV) → Pd(II) pathway (**INT-4** → **TS-4** → **INT-5**) has a merely 12.1 kcal·$mol^{-1}$ (energy barrier) and 11.6 kcal·$mol^{-1}$ (free energy barrier), indicating the intramolecular C−O bond-coupling through Pd(II) → Pd(0) to be extremely challenging with respect to the Pd(IV) → Pd(II) route. Despite both pathways being favorable overall in energy and free energy changes, these results support the Pd(II) → Pd(IV) → Pd(II) cycle as being the more kinetically probable one.

Toward resolving the widely differing reactivities of **INT-3** and **INT-4** with respect to the C−O RE process, the geometric and electronic structures (as molecular graphs generated by AIM analyses) of the relevant stationary points (**INT-3**, **INT-4**, **INT-4-b**, **INT-5**) and relevant transition structures (**TS-3**, **TS-3-b**) have been quantitatively and comparatively examined in detail (Figure 4); results show differences in geometric and electronic parameters in line with disparity in chemical behavior. For example, the Pd−O3 coordination bond in **TS-3-b** (2.67 Å) is substantially weakened relative to that in **INT-3** (2.23 Å), which is accompanied by lengthening of Pd−O4 from 2.17 to 2.30 Å. These structural changes are credible, as the change of oxidation state from +2 to 0 would result in the transformation of ligand field from a four-coordinate square to a two-coordinate linear configuration, which requires a labile spectator ligand (Pd−O3) departing from the Pd center upon the C−O bond-coupling. Similarly, there involves the change of ligand field from a six-coordinate octahedral to a four-coordinate square configuration accompanied by only a Pd−O3 lengthening from 2.33 Å in **INT-4** to 2.59 Å in **TS-4**. From the degree and the number of the weakened Pd−O coordinating bond, one can understand why the change of the ligand field structure from 6 → 4 coordination is more kinetically favorable than the 4 → 2 coordination change in the Pd complexes.

Analysis of the molecular graphs in Figure 4 shows the strong "key-lock" Pd−O coordination bonds in **INT-3** to all be of ionic nature with red nodal regions ($\nabla^2\rho > 0.0$) between Pd and O. All four bonds to Pd (Pd−O1/O3/O4/C6) weaken as the reaction proceeds **INT-3** → **TS-3-b**, the Pd−O3 coordination bond in particular ($\Delta\rho_b$ = (0.025 − 0.054) = (−0.029) $\bar{e}$·$bohr^{-3}$). In **TS-3-b**, the Pd−O1 and Pd−O3 bond paths pass through regions of electron-density concentration on the Pd atom (the 4 blue "oval lobes" in the valence density), enlarging the electronic-repulsion term. Contrastingly, in **INT-3**, they pass through areas of electron density depletion ("holes" in the blue valence density, where red nodal regions reach Pd's valence radius). This is indicative of the pseudo Pd(0) atom in **TS-3-b** being more electron-dense than the Pd(II) in **INT-3**. The augmented electron−electron repulsion between the central Pd and the O1 and O3 atoms in **TS-3-b** leads to longer Pd−O bond lengths, reducing stability in **TS-3-b** and a change of structure to pseudo-4-coordinated Pd.

As the reaction proceeds **INT-4** → **TS-4**, the six-coordinate structure is retained, in which bond strengths of Pd−O4 and Pd−O8 are slightly increased while the others are slightly decreased. This overall "give-take" equilibrating relationship furnishes **TS-4** with a low energy barrier, allowing the reaction to easily proceed to **INT-5**, which displays a stable planar-four-coordinate structure regenerating Pd(II).

**2.4. Role of Oxidant—INT-3x → INT-4x Transformation.** Toward quantitatively resolving the role of the oxidative $PhI(OAc)_2$ molecule (**2a**), the relative energies and free energies of an energetically plausible multistep oxidation mechanism have been determined using the B3LYP +IDSCRF/DZVP level of theory (Figure 5); here, **INT-3a** and **INT-4a** are the same as **INT-3** and **INT-4** discussed before since the exchange OAc− groups in **1a** are the same as those in **2a**. Our mechanistic pathway requires the two added acetate groups to be in *cis* orientation with respect to each other, consistent with an X-ray structural determination recently


dx.doi.org/10.1021/jo4010712 | J. Org. Chem. 2013, 78, 8376−8385

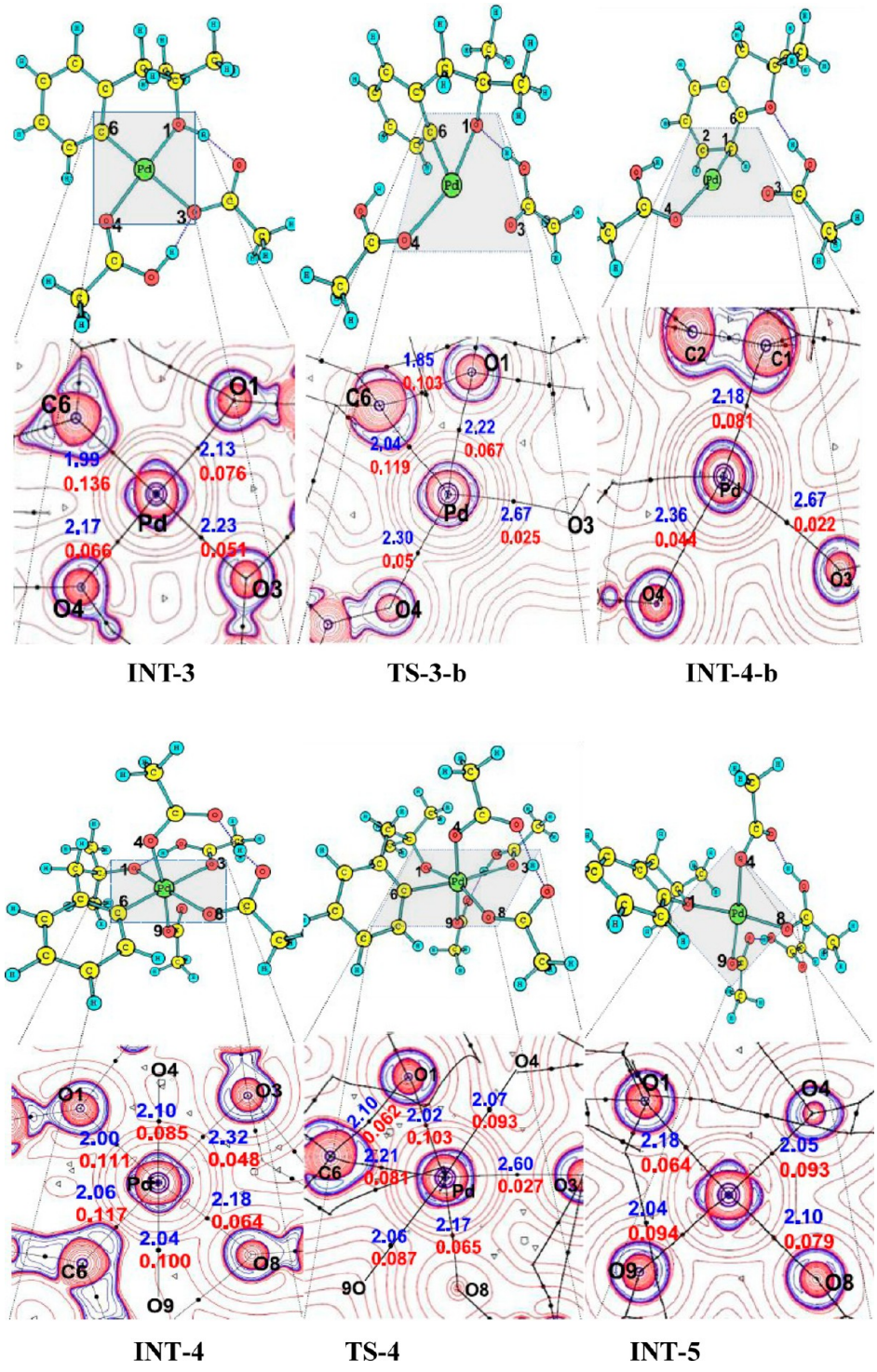


**Figure 4.** Principal Pd−O/C bond lengths (Å, blue text), bond paths (solid black lines), and electron densities ($\rho_b$ in au, red text) at bond critical points (small black dots). The "onion layer" 2-D isodensity surfaces were determined from the Laplacian of electron densities ($\nabla^2\rho$) in the plane of the Pd, O, and C atoms. Blue-lined regions represent electron concentration ($\nabla^2\rho < 0.0$), corresponding to core and valence electronic density around each atoms. Red-lined regions represent electron depletion ($\nabla^2\rho > 0.0$) and correspond to nodal regions.

reported for the oxidation product of a Pd(II) complex with **2a**.[13a]

Prior to oxidizing Pd(II) to Pd(IV), **INT-3a** must first exchange its coordinating acetic acid O4 atom with the acetate O7 atom of **2a** via a concerted transition state (**OX-TS-1a**), affording another square Pd(II) intermediate (**OX-INT-1a**), with a near-negligible energy and free energy barriers of +8.1 and +9.9 kcal·mol$^{-1}$, respectively.

This is followed by the **OX-TS-2a** transition state with +30.8 and +30.9 kcal·mol$^{-1}$ energy and free energy barriers, respectively, both accessible at the experimental temperature (373 K). In the **OX-TS-2a** structure, O9 of the PhI(OAc) moiety and O4 in acetic acid attack the Pd center from axial directions, with bond distances of Pd−O9, Pd−O4, O8−I, and O10−I being 2.42, 2.79, 2.73 and 2.51 Å, respectively. The imaginary vibrational mode of **OX-TS-2a** shows the O8−I and


dx.doi.org/10.1021/jo4010712 | J. Org. Chem. 2013, 78, 8376−8385

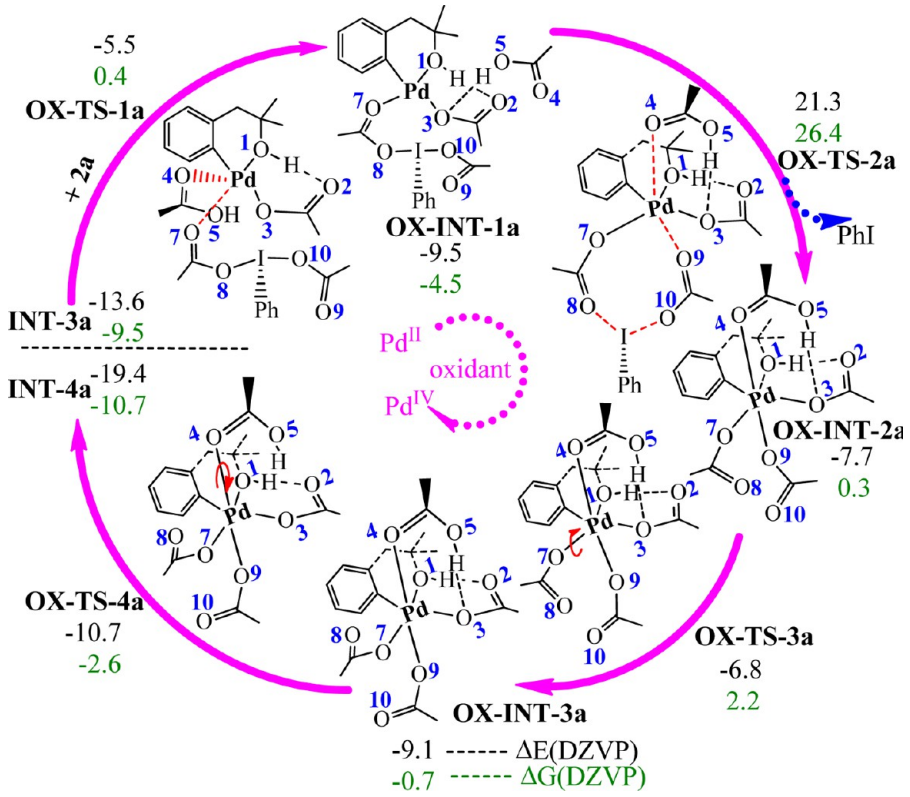


**Figure 5.** Depiction of the geometry-optimized (stable) structures along the putative mechanistic pathway for the **INT-3a** + **2a** → **INT-4a** + PhI oxidation process. Weakly polar interactions are indicated by dashed bond lines, in addition to atomic numbering used (blue text) and the relative energies and free energies (kcal·mol$^{-1}$) as determined at the B3LYP+IDSCRF/DZVP level of theory.

**Table 1. Comparison of Experimental Yields with Relative Energies and Free Energies (kcal·mol$^{-1}$) for the INT-3x + 2x → INT-4x + RED-x (x = a−e) Chemical Transformation, For Differing Oxidants, As Determined by the B3LYP+IDSCRF/DZVP and B3LYP+IDSCRF/TZVP+SDD Levels of Theory**

| | | DZVP | | TZVP+SDD | |
|---|---|---|---|---|---|
| oxidant [equiv] | yield (%) | Δ*E* | Δ*G* | Δ*E* | Δ*G* |
| $PHI(OAc)_2$ (**2a**) [1.5] | 88 | −5.8 | −1.2 | −22.9 | −17.7 |
| $PHI(TFA)_2$ (**2b**) [1.5] | 13 | −2.3 | +2.6 | −18.9 | −13.5 |
| $PHI(OPiv)_2$ (**2c**) [1.5] | 50 | −5.5 | +1.0 | −21.4 | −16.5 |
| AgOAc (**2d**) [3.0] | 0 | +53.1 | +74.7 | | |
| $Cu(OAc)_2$ (**2e**) [1.5] | 0 | +12.4 | +33.3 | | |

O10−I distances becoming longer, while those of Pd−O9 and Pd−O4 become smaller; departure of the PhI species allows formation of the 6-coordinate Pd(IV) intermediate **OX-INT-2a**.

To complete the oxidation process leading to **INT-4a**, the H atom involved in the O5−H···O3 intramolecular interaction must be transferred to O8, forming the O8···H−O5 H-bond. This occurs via the following two-step process: **OX-INT-2a** → **OX-TS-3a** → **OX-INT-3a**, followed by **OX-INT-3a** → **OX-TS-4a** → **INT-4a**. The first step has total energy and free energy barriers of +0.9 and +1.9 kcal·mol$^{-1}$, respectively, while the second step has negative energy and free energy barriers of −1.6 and −1.9 kcal·mol$^{-1}$, respectively. These barriers are both easily surmounted at 373 K; hence, both steps effecting H-transfer proceed easily under experimental conditions. Although **OX-TS-4a** is slightly lower in total energy and free energy than its precursor (**OX-INT-3a**), the pure electronic energy data showed it to be 0.3 kcal·mol$^{-1}$ higher in electronic energy than the preceding **OX-INT-3a** structure after subtracting zero-point energies (ZPEs) from total energies. Refinement of theoretical approximations, including use of anharmonic potentials, or very resource-intensive quantification of dispersion effects, would allow improvement of energetic determinations for these highly networked complexes. We have also found the similar reaction path **INT-3b** + **2b** → **INT-4b** + PhI (see the Supporting Information), and the free energy barrier for the rate-determining step of **OX-INT-1b** → **OX-INT-2b** + PhI is only 26.2 kcal·mol$^{-1}$, ca. 4.7 kcal·mol$^{-1}$ lower than that for oxidant (**2a**), indicating that these steps are not kinetically controlled as these barriers are accessible at the experimental temperature used (373 K). The most plausible reason, therefore, is that the thermal equilibrium between **INT-3x** and **INT-4x** plays a pivotal role on the dependence of oxidants.

Experimentally determined product yields for C−O bond formation show the process as being highly dependent on oxidant identity (Table 1). The agreement between experimental yields and the theoretically determined relative energy


dx.doi.org/10.1021/jo4010712 | J. Org. Chem. 2013, 78, 8376−8385

and free energy barriers provides strong support to our proposal that Pd(II) → Pd(IV) oxidation presents an energetically accessible channel for the C−O RE process.

In general, oxidation of Pd(0) → Pd(II) is relatively easy, as various kinds of oxidants, such as benzoquinone, $(^tBuO)_2$, acetic peracid, $Cu(OAc)_2$, AgF, $K_2S_2O_8$, and $O_2$, are adequate to oxidize Pd(0) complexes to Pd(II) complexes in solution. In contrast, oxidation of Pd(II) → Pd(IV) is traditionally considered to be energetically challenging due to the instability of Pd(IV) structures in solution—hence the requisite powerful oxidants.

Experiments show **2a** to be the best choice of oxidant to include for the studied reaction (Table 1); formation of the Pd(IV) intermediate (**INT-4a**) is favorable. Energy and free energy changes for the oxidation process (**INT-3a** → **INT-4a**) are −5.8 and −1.2 kcal·mol$^{-1}$, respectively. For other oxidants, their free energy changes are all positive, meaning that the Pd(II) intermediate (**INT-3x**) is favored at this equilibrium point in the reaction. This is particularly true for the AgOAc and $Cu(OAc)_2$ oxidants, where the **INT-3x** → **INT-4x** process would not proceed. However, the TZVP+SDD basis set predicts lower reaction total energies and free energies by ca. 16−18 kcal·mol$^{-1}$ for three oxidants (**2a**, **2b**, and **2c**), regardless of the DFT functionals used (CAM-B3LYP, M06, and wb97xD; see the Supporting Information). We believe that this difference originates from the pseudopotential basis set as the SDD pseudopential for Pd was derived from the neutral Pd atom, and is identical for any other oxidation states. Such an approximation is clearly erroneous (even to nonspecialists) to characterize a reaction involving a Pd(II) ↔ Pd(IV) change; an all-electron basis set should be employed for such cases.

## 3. CONCLUSIONS

Density functional theory determinations, employing the B3LYP+IDSCRF/DZVP and B3LYP+IDSCRF/BS1 levels, have been employed to qualitatively characterize the thermodynamic and kinetic aspects of a $Pd(OAc)_2$-catalyzed C−H activation/C−O cyclization. The following conclusions have been reached:

(1) The Pd(II) → Pd(IV) → Pd(II) catalytic cycle involving a Pd(IV) intermediary species is determined to be the most energetically plausible reaction pathway, in which an oxidation process of Pd(II) → Pd(IV) precedes the C−O reductive elimination process.

(2) The Pd(II) → Pd(0) step in the C−O reductive elimination process, within the Pd(II) → Pd(0) → Pd(II) cycle, is kinetically unfavorable with an energy barrier of 41.0 kcal·mol$^{-1}$.

(3) The yield of final product is dependent on the relative stability of the Pd(IV) intermediate (**INT-4**) within the Pd(II) → Pd(IV) → Pd(II) cycle—itself highly dependent on the nature of the oxidant employed.

## 4. COMPUTATIONAL DETAILS

All calculations in this work were performed with the B3LYP method as implemented in the Gaussian 09 program package (G09),[17] employing the standard double-$\zeta$ valence polarized (DZVP) all-electron basis set for all atoms.[18] The self-consistent reaction field (SCRF) polarizable continuum model (PCM)[19] was used to calculate the solvent effect of perfluorobenzene ($\varepsilon$ = 2.029). Atomic radii were defined with the IDSCRF method[20] (denoted B3LYP+IDSCRF herein) to more accurately quantify the spatial extent of the molecular cavity.

All structures residing at stationary points identified were subsequently characterized by frequency analyses, from which their (relative) free energies were obtained, in addition to verifying the stationary points to be the minima or first-order saddle points on the potential energy surface. Intrinsic reaction coordinate (IRC)[21] calcu-calculations with the Hessian-based predictor−corrector integrator (HPC)[22] were also used to confirm selected transition-state structures as connecting the two adjacent minima on their respective potential energy hypersurfaces.

For comparative purpose, selected stationary points have been reoptimized and characterized with a mixed basis set (BS1), in which TZVP[23] was used for C, H, and O atoms and ECP(SDD)[24] was used for Pd and I atoms. The total energies reported in this paper have been corrected with zero-point energies (ZPEs), and the Gibbs free energies have also been corrected to be consistent with the experimental temperature of 373 K.

To test the effect of differing functionals, the CAM-B3LYP,[25] M06,[26] and wb97xD[27] methods have been employed to characterize the main stationary points for the C−H activation process; single point energy corrections have been performed. For the **INT-3x** → **INT-4x** (**x** = **a**, **b**, **c**) transformation, the geometric parameters for related stationary points have been reoptimized and frequencies have been obtained with corresponding methods.

The electronic structures of selected structures were analyzed by Bader's atoms-in-molecules (AIM) analyses, to quantitatively characterize the topological properties of the electron density distributions.[28] Analyses were carried out on the wave functions generated using the B3LYP+IDSCRF/DZVP method on the geometry-optimized structures. All molecular graphs and 2-dimensional Laplacian reported in this article have been performed with the AIM98PC[29] program package, a modified version of the AIMPAC program.[30]

## ■ ASSOCIATED CONTENT

### Supporting Information

The Supporting Information contains the following data: optimized Cartesian coordinates for all stationary points; vibrational frequencies; total energies, zero-point energies, and total free energies; and complementary mechanistic characterizations for oxidation process. This material is available free of charge via the Internet at http://pubs.acs.org.

## ■ AUTHOR INFORMATION

### Corresponding Author

*E-mail: dcfang@bnu.edu.cn.

### Notes

The authors declare no competing financial interest.

## ■ ACKNOWLEDGMENTS

This work was supported by the National Nature Science Foundation of China (21073016). G.A.C. and D.-C.F. thank the Royal Society (project IE120096) and GIOCOMMS (Toronto/Budapest/Beijing) for supporting international research exchanges. G.A.C. acknowledges the support of the EPSRC (EP/H030077/1, EP/H030077/2) and STFC, U.K.

## ■ REFERENCES

(1) (a) Ryabov, A. D. *Chem. Rev.* **1990**, *90*, 403−424. (b) Bergman, R. G. *Nature* **2007**, *466*, 391−393. (c) Park, Y. J.; Park, J. W. P.; Jun, C. H. *Acc. Chem. Res.* **2008**, *41*, 222−234. (d) Godula, K.; Sames, D. *Science* **2006**, *312*, 67−72. (e) Crabtree, R. H. *Chem. Rev.* **1985**, *85*, 245−269.

(2) (a) Hartwig., J. F. *Nature* **2008**, *455*, 314−322. (b) Kalyani, D.; Deprez, N. R.; Desai, L. V. *J. Am. Chem. Soc.* **2005**, *127*, 7330−7331. (c) Muci, A. R.; Buchwald, S. L. *Top. Curr. Chem.* **2002**, *219*, 131−209. (d) Hartwig, J. F. *Inorg. Chem.* **2007**, *46*, 1936−1947. (e) Arndtsen, B. A.; Bergman, R. G.; Mobley, T. A.; Peterson, T. H. *Acc. Chem. Res.*

**1995**, *28*, 154−162. (f) Echavarren, A. *Angew. Chem. Int. Ed.* **2004**, *116*, 4808−4839. (g) Colby, D. A.; Bergman, R. G.; Ellman, J. A. *Chem. Rev.* **2010**, *110*, 624−655.
(3) (a) Lyons, T. W.; Sanford, M. S. *Chem. Rev.* **2010**, *110*, 1147−1169. (b) Chen, X.; Engle, K. M.; Wang, D. H.; Yu, J. Q. *Angew. Chem. Int. Ed.* **2009**, *48*, 5094−5115.
(4) (a) Dick, A. R.; Sanford, M. S. *Tetrahedron* **2006**, *62*, 2439−2463. (b) Thu, H. Y.; Yu, W. Y.; Che, C. M. *J. Am. Chem. Soc.* **2006**, *128*, 9048−9049. (c) Mei, T. S.; Wang, X.; Yu, J. Q. *J. Am. Chem. Soc.* **2009**, *131*, 10806−10807.
(5) (a) Shi, L.; Tu, Y. Q.; Wang, M. *Org. Lett.* **2004**, *6*, 1001−1003. (b) Fiedler, D.; van Halbeek, H.; Bergman, R. G. *J. Am. Chem. Soc.* **2006**, *128*, 10240−10252. (c) Lu, Y.; Wang, D. H.; Engle, K. M.; Yu, J. Q. *J. Am. Chem. Soc.* **2010**, *132*, 5916−5921. (d) He, L.; Yu, J.; Zhang, J.; Yu, X.-Q. *Org. Lett.* **2007**, *9*, 2277−2280. (e) Kawai, H.; Kobayshi, Y.; Oi, S.; Inoue, Y. *Chem. Commun.* **2008**, 1464−1466.
(6) (a) Lim, S. G.; Ahn, J. A.; Jun, C. H. *Org. Lett.* **2004**, *6*, 4687−4690. (b) Jordan-Hore, J. A.; Johansson, C. C.; Gulias, C. M.; Beck, E. M.; Gaunt, M. J. *J. Am. Chem. Soc.* **2008**, *130*, 16184−16186. (c) Wasa, M.; Yu, J. Q. *J. Am. Chem. Soc.* **2008**, *130*, 14058−14059.
(7) (a) Ritleng, V.; Sirlin, C.; Pfeffer, M. *Chem. Rev.* **2002**, *102*, 1731−1770. (b) Klei, S. R.; Tilley, T. D.; Bergman, R. G. *J. Am. Chem. Soc.* **2000**, *122*, 1816−1817. (c) Xi, Z.; Liu, B.; Chen, W. J. *Org. Chem.* **2008**, *73*, 3954−3957. (d) Siegbahn, P. E. M.; Crabtree, R. H. *J. Am. Chem. Soc.* **1997**, *119*, 3103−3113. (e) Fukuyama, T.; Shinmen, M.; Nishitani, S. *Org. Lett.* **2002**, *4*, 1691−1694. (f) Hagiwara, I.; Sugawara, Y.; Isobe, K.; Suzuki, T. *Org. Lett.* **2004**, *6*, 2325−2328.
(8) (a) Cho, J. Y.; Iverson, C. N.; Smith, M. R. *J. Am. Chem. Soc.* **2000**, *122*, 12868−12869. (b) Lafrance, M.; Rowley, C. N.; Woo, T. K.; Fagnou, K. *J. Am. Chem. Soc.* **2006**, *128*, 8754−8756. (c) Maseras, F.; Echavarren, A. M. *J. Am. Chem. Soc.* **2006**, *128*, 1066−1067. (d) Jia, C.; Piao, D.; Oyamada, J. *Science* **2000**, *287*, 1992−1995. (e) Stuart, D. R.; Villemure, E.; Fagnou, K. *J. Am. Chem. Soc.* **2007**, *129*, 12072−12073. (f) Zhou, W.; Wang, L. *Org. Lett.* **2012**, *14*, 4594−4597.
(9) (a) Cho, S. H.; Kim, J. Y.; Kwak, J. *Chem. Soc. Rev.* **2011**, *40*, 5068−5083. (b) Tani, M.; Sakaguchi, S.; Ishii, Y. J. *Org. Chem.* **2004**, *69*, 1221−1226. (c) Davies, H. M. L.; Jin, Q.; Ren, P. *J. Org. Chem.* **2002**, *67*, 4165−4169. (d) Desai, L. V.; Hull, K. L.; Sanford, M. S. *J. Am. Chem. Soc.* **2004**, *126*, 9542−9543. (e) Kalyani, D.; Sanford, M. S. *Org. Lett.* **2005**, *7*, 4149−4152. (f) Torborg, C.; Beller, M. *Adv. Synth. Catal.* **2009**, *351*, 3027−3043. (g) King, A. O.; Yasuda, N. *Organomet. Process Chem.* **2004**, *6*, 205−245. (h) Magano, J.; Dunetz, J. R. *Chem. Rev.* **2011**, *111*, 2177−2250. (i) Evano, G.; Blanchard, N.; Toumi, M. *Chem. Rev.* **2008**, *108*, 3054−3131. (j) Kakiuchi, F.; Kochi, T. *Synthesis* **2008**, 3013−3039.
(10) (a) Pytkowicz, J.; Roland, S.; Mangeney, P. *J. Organomet. Chem.* **2003**, *678*, 166−179. (b) Lebel, H.; Janes, M. K.; Charette, A. B.; Nolan, S. P. *J. Am. Chem. Soc.* **2004**, *126*, 5046−5047. (c) Wang, D. H.; Mei, T. S.; Yu, J. Q. *J. Am. Chem. Soc.* **2008**, *130*, 17676−17677. (d) Miyaura, N.; Yamada, K.; Suzuki, A. *Tetrahedron Lett.* **1979**, 3437−3440. (e) Nadres, E. T.; Daugulis, O. *J. Am. Chem. Soc.* **2011**, *134*, 7−10. (f) Giri, R.; Maugel, N.; Li, J. J.; Wang, D. H.; Breazzano, S. P.; Saunders, L. B.; Yu, J. Q. *J. Am. Chem. Soc.* **2007**, *129*, 3510−3511. (g) Mkhalid, I. A.; Barnard, J. H.; Marder, T. B.; Murphy, J. M.; Hartwig, J. F. *Chem. Rev.* **2010**, *110*, 890−931. (h) Marciniec, B.; Majchrzak, M.; Prukala, W.; Kubicki, M.; Chadyniak, D. *J. Org. Chem.* **2005**, *70*, 8550−8555. (i) Chu, J. H.; Chen, C. C.; Wu, M. J. *Organometallics* **2008**, *27*, 5173−5176. (j) Srimani, D.; Bej, A.; Sarkar, A. *J. Org. Chem.* **2010**, *75*, 4296−4299. (k) Ge, H.; Niphakis, M. J.; Georg, G. I. *J. Am. Chem. Soc.* **2008**, *130*, 3708−3709. (l) Hiyama, T. *J. Organomet. Chem.* **2002**, *653*, 58−61. (m) Chen, X.; Goodhue, C. E.; Yu, J. Q. *J. Am. Chem. Soc.* **2006**, *128*, 12634−12635. (n) Hartwig, J. F. *Chem. Soc. Rev.* **2011**, *40*, 1992−2002.
(11) (a) Zhang, Y. H.; Shi, B. F.; Yu, J. Q. *J. Am. Chem. Soc.* **2009**, *131*, 5072−5074. (b) Dick, A. R.; Hull, K. L.; Sanford, M. S. *J. Am. Chem. Soc.* **2004**, *126*, 2300−2301. (c) Desai, L. V.; Malik, H. A.; Sanford, M. S. *Org. Lett.* **2006**, *8*, 1141−1144. (d) Lu, Y.; Wang, D. H.; Engle, K. M. *J. Am. Chem. Soc.* **2010**, *132*, 5916−5921. (e) Desai, L. V.; Hull, K. L.; Sanford, M. S. *J. Am. Chem. Soc.* **2004**, *126*, 9542−9543. (f) Shelby, Q.; Kataoka, N.; Mann, G.; Hartwig, J. F. *J. Am. Chem. Soc.* **2000**, *122*, 10718−10719. (g) Kuwabe, S.; Torraca, K. E.; Buchwald, S. L. *J. Am. Chem. Soc.* **2001**, *123*, 12202−12206. (h) Maimone, T. J.; Buchwald, S. L. *J. Am. Chem. Soc.* **2010**, *132*, 9990−9991.
(12) (a) Livendahl, M.; Echavarren, A. M. *Isr. J. Chem.* **2010**, *50*, 630−651. (b) García-Cuadrado, D.; et al. *J. Am. Chem. Soc.* **2006**, *128*, 1066−1067. (c) García-Cuadrado, D.; Echavarren, A. M. *J. Am. Chem. Soc.* **2007**, *129*, 6880−6886. (d) Davies, D. L.; Donald, S. M. A.; Macgregor, S. A. *J. Am. Chem. Soc.* **2005**, *127*, 13754−13755. (e) Ke, Z.; Cundari, T. R. *Organometallics* **2010**, *29*, 821−834. (f) Furuya, T.; Benitez, D.; Tkatchouk, E. *J. Am. Chem. Soc.* **2010**, *132*, 3793−3807. (g) Bielsa, R.; Navarro, R.; Urriolabeitia, E. P.; Lledos, A. *Inorg. Chem.* **2007**, *46*, 10133−10142. (h) Mota, J.; Dedieu, A. *Organometallics* **2006**, *25*, 3130−3142.
(13) (a) Byers, P. K.; Canty, A. J.; Skelton, B. W. *J. Chem. Soc., Chem. Commun.* **1986**, 1722−1724. (b) Canty, A. J. *Acc. Chem. Res.* **1992**, *25*, 83−90. (c) Hickman, A. J.; Sanford, M. S. *Nature* **2012**, *484*, 177−185. (d) Dick, A. R.; Kampf, J. W.; Sanford, M. S. *J. Am. Chem. Soc.* **2005**, *127*, 12790−12791. (e) Welbes, L. L.; Lyons, T. W.; Cychosz, K. A.; Sanford, M. S. *J. Am. Chem. Soc.* **2007**, *129*, 5836−5837. (f) Hull, K. L.; Lanni, E. L.; Sanford, M. S. *J. Am. Chem. Soc.* **2006**, *128*, 14047−14049. (g) Muñiz, K. *Angew. Chem., Int. Ed.* **2009**, *48*, 9412−9423. (h) Wang, X.; Leow, D.; Yu, J. Q. *J. Am. Chem. Soc.* **2011**, *133*, 13864−13867. (i) Pilarski, L. T.; Selander, N.; Bose, D.; Szabo, K. J. *Org. Lett.* **2009**, *11*, 5518−5521. (j) Racowski, J. M.; Gary, B. G.; Sanford, M. S. *Angew. Chem., Int. Ed.* **2012**, *51*, 3414−3417. (k) Racowski, J. M.; Ball, N. D.; Sanford, M. S. *J. Am. Chem. Soc.* **2011**, *133*, 18022−18025. (l) Hickman, A. J.; Sanford, M. S. *ACS Catal.* **2011**, *1*, 170−174. (m) Sibbald, P. A.; Rosewall, C. F.; Swartz, R. D.; Michael, F. E. *J. Am. Chem. Soc.* **2009**, *131*, 15945−15951.
(14) Wang, X. S.; Yu, J. Q. *J. Am. Chem. Soc.* **2010**, *132*, 12203−12205.
(15) Parr, R. G.; Yang, W. *Density-Functional Theory of Atoms and Molecules*; Oxford University Press: New York, 1989.
(16) Whisler, M. C.; MacNeil, S.; Snieckus, V.; Beak, P. *Angew. Chem., Int. Ed.* **2004**, *43*, 2206−2225.
(17) Frisch, M. J.; Trucks, G. W.; Schlegel, H. B.; Scuseria, G. E.;Robb, M. A.; Cheeseman, J. R.; Scalmani, G.; Barone, V.; Mennucci, B.; Petersson, G. A.; Nakatsuji, H.; Caricato, M.; Li, X.; Hratchian, H. P.; Izmaylov, A. F.; Bloino, J.; Zheng, G.; Sonnenberg, J. L.; Hada, M.;Ehara, M.; Toyota, K.; Fukuda, R.; Hasegawa, J.; Ishida, M.; Nakajima,T.; Honda, Y.; Kitao, O.; Nakai, H.; Vreven, T.; Montgomery, J. A., Jr.; Peralta, J. E.; Ogliaro, F.; Bearpark, M.; Heyd, J. J.; Brothers, E.; Kudin,K. N.; Staroverov, V. N.; Kobayashi, R.; Normand, J.; Raghavachari, K.;Rendell, A.; Burant, J. C.; Iyengar, S. S.; Tomasi, J.; Cossi, M.; Rega,N.; Millam, J. M.; Klene, M.; Knox, J. E.; Cross, J. B.; Bakken, V.;Adamo, C.; Jaramillo, J.; Gomperts, R.; Stratmann, R. E.; Yazyev, O.;Austin, A. J.; Cammi, R.; Pomelli, C.; Ochterski, J. W.; Martin, R. L.;Morokuma, K.; Zakrzewski, V. G.; Voth, G. A.; Salvador, P.;Dannenberg, J. J.; Dapprich, S.;Daniels, A. D.; Farkas,O.; Foresman, J. B.; Ortiz, J. V.; Cioslowski, J.; Fox, D. J. *Gaussian 09*, Revision A.02; Gaussian, Inc.: Wallingford, CT, 2009.
(18) (a) Godbout, N.; Salahub, D. R.; Andzelm, J.; Wimmer, E. *Can. J. Chem.* **1992**, *70*, 560−571. (b) Sosa, C.; Lee, C. *J. Phys. Chem.* **1992**, *96*, 6630−6636.
(19) Scalmani, G.; Frisch, M. J. *J. Chem. Phys.* **2010**, *132*, 114110−114124.
(20) (a) Tao, G. Y.; Mu, W. H.; Chass, G. A.; Tang, T.-H.; Fang, D.-C. *Int. J. Quantum Chem.* **2013**, *113*, 975−984. (b) Fang, D.-C. *SCRF-RADII*; Beijing Normal University: Beijing, China, free of charge for academic users.
(21) Fukui, K. *Acc. Chem. Res.* **1981**, *14*, 363−368.
(22) (a) Hratchian, H. P.; Schlegel, H. B. *J. Chem. Phys.* **2004**, *120*, 9918−9924. (b) Hratchian, H. P.; Schlegel, H. B. *J. Chem. Theory Comput.* **2005**, *1*, 61−69.
(23) Schaefer, A.; Huber, C.; Ahlrichs, R. *J. Chem. Phys.* **1994**, *100*, 5829−5835.
(24) Andrae, D.; Haeussermann, U.; Dolg, M.; Stoll, H.; Preuss, H. *Theor. Chim. Acta* **1990**, *77*, 123−141.

(25) Yanai, T.; Tew, D.; Handy, N. *Chem. Phys. Lett.* **2004**, *393*, 51−57.
(26) Zhao, Y.; Truhlar, D. G. *Theor. Chem. Acc.* **2008**, *120*, 215−241.
(27) Chai, J.-D.; Head-Gordon, M. *J. Chem. Phys.* **2008**, *128*, 084106.
(28) Bader, R. F.W. *Atoms in Molecules: A Quantum Theory*; Oxford University Press: Oxford, UK, 1990.
(29) Fang, D.-C.; Tang, T.-H. *AIM98PC*; Beijing Normal University: Beijing, China, 1998.
(30) *AIMPAC*, available from Professor Bader's Laboratory; McMaster University: Hamilton, Ontario, Canada.